

## Tchnetium(IV) Halides Predicted from First-Principles

Philippe F. Weck,<sup>\*,†</sup> Eunja Kim,<sup>‡</sup> Frédéric Poineau,<sup>†</sup> Efrain E. Rodriguez,<sup>§</sup> Alfred P. Sattelberger,<sup>||</sup> and Kenneth R. Czerwinski<sup>†</sup>

<sup>†</sup>Department of Chemistry and Harry Reid Center for Environmental Studies and <sup>‡</sup>Department of Physics and Astronomy and University of Nevada Las Vegas, 4505 Maryland Parkway, Las Vegas, Nevada 89154,

<sup>§</sup>Lujan Neutron Scattering Center, Los Alamos National Laboratory, Los Alamos, New Mexico 87545, and

<sup>||</sup>Energy Sciences and Engineering Directorate, Argonne National Laboratory, Argonne, Illinois 60439

Received March 11, 2009

We report the crystal structures of the novel technetium tetrahalides  $TcX_4$  [ $X = F, I$ ], as predicted from first-principles calculations. Isomorphous with  $TcCl_4$  and  $TcBr_4$  crystals,  $TcF_4$  is orthorhombic with the centro-symmetric space group  $Pbca$ , while  $TcI_4$  crystallizes in the monoclinic space group  $P2_1/c$ . The structures,  $[TcX_2(\mu-X)_{4/2}]_\infty$ , consist of distorted edge-sharing octahedral groups of composition  $TcX_6$  linked into endless *cis* chains. A possible explanation for the differences between these structures is offered in terms of varying degrees of bonding within the chains.

### Introduction

Metal halides and their derivatives commonly form oligomers and polymers.<sup>1–3</sup> In particular, metal halides of composition  $MX_4$  show a propensity to form chains consisting of  $MX_6$  edge-sharing octahedra, with *cis* or *trans* arrangements of the non-bridging X atoms.<sup>4</sup>

Among tetrahalides of the stable manganese group elements (Mn, Tc, and Re), the crystal structure of  $TcCl_4$  was the first to be unambiguously established.<sup>5,6</sup>  $TcCl_4$  crystallizes in the orthorhombic centro-symmetric space group  $Pbca$ , with four chains per unit cell (cf. Figure 1). The repeating unit of the chains is a  $Tc_2Cl_8$  moiety made up of two  $TcCl_4$  planar asymmetric units related to each other by a glide plane, resulting in  $[TcCl_2(\mu-Cl)_{4/2}]_\infty$  *cis* chains,<sup>4</sup> similar to  $ZrCl_4$ ,<sup>7</sup>  $PtCl_4$ ,<sup>8</sup>  $PtI_4$ ,<sup>9</sup> and  $UI_4$ .<sup>10</sup> The crystal structure of  $TcCl_4$  may be contrasted with the structure of  $ReCl_4$  ( $\beta$  phase, space group  $P2/c$ ) characterized by Cotton and co-workers.<sup>11,12</sup>

The latter compound is composed of zigzag chains of  $Re_2Cl_9$  confacial bioctahedra, in which one terminal Cl atom at each end is shared between two bioctahedra, that is,  $[ReCl_2(\mu-Cl)_{3/2}(\mu-Cl)_{1/2}]_\infty$ . This structure allows the formation of a Re–Re bond of 2.73 Å across the shared octahedral face,<sup>12</sup> while in  $TcCl_4$  chains the Tc–Tc distance of 3.62 Å and the angles in the inner chloro bridge rhomboids indicate that Tc atoms are repelling each other.<sup>6</sup>

Isomorphous with  $TcCl_4$ ,  $TcBr_4$  is the only other known technetium tetrahalide compound and was recently synthesized and characterized by single crystal X-ray diffraction (XRD).<sup>13</sup> This lack of information on Tc(IV) halides illustrates the immaturity of Tc coordination chemistry, most of which is oriented toward the development of <sup>99m</sup>Tc-based agents for radiopharmaceutical imaging.<sup>14,15</sup> Recent synthetic advances have demonstrated the benefit of using  $TcCl_4$  as starting material for the preparation of *cis*- $[TcCl_4(L)_2]$  complexes, which can be used as precursors for further reactions with chelating ligands to obtain new classes of Tc(IV) complexes.<sup>16</sup> New technetium halide compounds such as  $TcBr_4$  open up opportunities for further research in synthetic Tc chemistry.

In this paper, we report the crystal structures of technetium tetrafluoride ( $TcF_4$ ) and tetraiodide ( $TcI_4$ ) as predicted from density functional theory (DFT) calculations. The structures of  $TcCl_4$  and the recently synthesized  $TcBr_4$  compound are also investigated computationally and compared with available

\*To whom correspondence should be addressed. E-mail: weckp@unlv.nevada.edu.

(1) Wyckoff, R. W. *Crystal Structures*; Wiley-Interscience: New York, 1965; Vols. 1–3.

(2) Gutman, V. *Halogen Chemistry*; Academic Press: New York, 1967; Vol. 3.

(3) Corbett, J. D. *Acc. Chem. Res.* **1981**, *14*, 239.

(4) Müller, V. U. *Acta Crystallogr.* **1981**, *B37*, 532.

(5) Elder, M.; Penfold, B. R. *Chem. Commun.* **1965**, *14*, 308.

(6) Elder, M.; Penfold, B. R. *Inorg. Chem.* **1966**, *5*, 1197.

(7) Krebs, B. *Z. Anorg. Allg. Chem.* **1970**, *378*, 263.

(8) Pilbrow, M. F. *Chem. Commun.* **1978**, *S*, 270.

(9) Brodersen, K.; Thiele, G.; Holle, B. *Z. Anorg. Allg. Chem.* **1969**, *369*, 154.

(10) Levy, J. H.; Taylor, J. C.; Wugh, A. B. *Inorg. Chem.* **1980**, *19*, 672.

(11) Bennett, M. J.; Cotton, F. A.; Foxman, B. M.; Stokely, P. F. *J. Am. Chem. Soc.* **1967**, *89*, 2759.

(12) Cotton, F. A.; DeBoer, B. G.; Mester, Z. *J. Am. Chem. Soc.* **1973**, *95*, 1159.

(13) Poineau, F.; Rodriguez, E. E.; Forster, P. M.; Sattelberger, A. P.; Cheetham, A. K.; Czerwinski, K. R. *J. Am. Chem. Soc.* **2009**, *131*, 910.

(14) Storr, T.; Thompson, K. H.; Orvig, C. *Chem. Soc. Rev.* **2006**, *35*, 534.

(15) Tisato, F.; Porchia, M.; Bolzati, C.; Refosco, F.; Vittadini, A. *Coord. Chem. Rev.* **2006**, *250*, 2034.

(16) Hagenbach, A.; Yegen, E.; Abram, U. *Inorg. Chem.* **2006**, *45*, 7331.

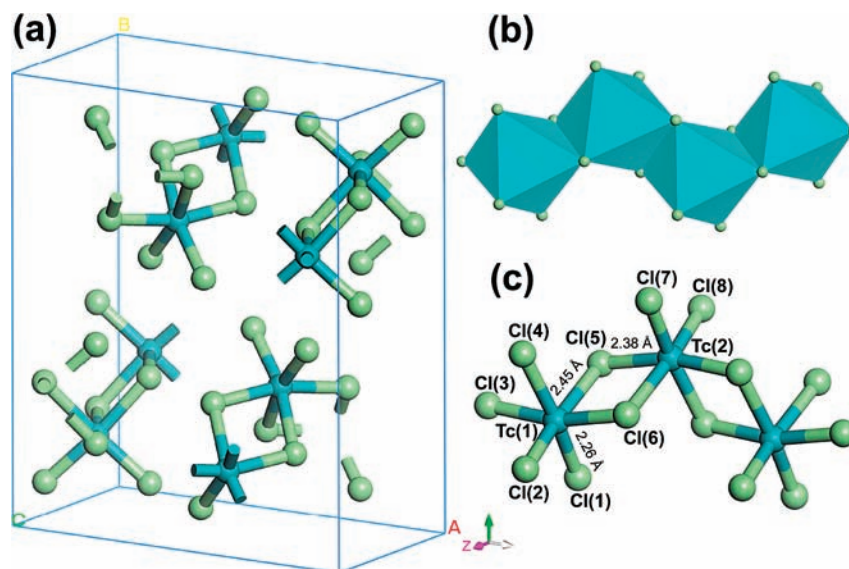


**Figure 1.** Ball-and-stick models of the computed equilibrium structure of technetium(IV) chloride: (a) Unit cell of the  $\text{TcCl}_4$  crystal with orthorhombic space group  $Pbc_a$ ; (b)  $\text{TcCl}_4$  chain of edge-sharing octahedra with *cis* arrangements of the non-bridging Cl atoms; (c) distorted octahedra with three distinct Tc–Cl bonds.

experimental data. A possible explanation for the differences between Tc tetrahalide structures is also discussed in terms of varying degrees of bonding within the chains. Details of our computational approach are given in the next section, followed by a discussion and analysis of our results. A summary of our findings and conclusions are given in the last section.

### Computational Methods

First-principles all-electron calculations of the total energies and optimized geometries were performed using the spin-polarized density functional theory as implemented in the DMol3 software.<sup>17</sup> The exchange correlation energy was calculated using the generalized gradient approximation (GGA) employing the Perdew–Wang (PW91) density functional.<sup>18</sup> Double numerical basis sets including polarization functions on all atoms (DNP) were used in the calculations. The DNP basis set corresponds to a double- $\zeta$  quality basis set with a p-type polarization function added to hydrogen and d-type polarization functions added to heavier atoms. The DNP basis set is comparable to 6-31G\*\* Gaussian basis sets<sup>19</sup> with a better accuracy for a similar basis set size.<sup>17</sup> In the generation of the numerical basis sets, a global orbital cutoff of 4.8 Å was used.

The energy tolerance in the self-consistent field calculations was set to  $10^{-6}$  Hartree. Optimized geometries were obtained using the direct inversion in a subspace method (DIIS) without symmetry constraints with an energy convergence tolerance of  $10^{-5}$  Hartree and a gradient convergence of  $2 \times 10^{-3}$  Hartree/Bohr. The working unit cells contain 8 Tc atoms and 32 halide atoms. The Brillouin zone was sampled using the Monkhorst–Pack special  $k$ -point scheme<sup>20</sup> with a  $2 \times 2 \times 4$  mesh for structural optimization and total energy calculations.

### Results and Discussion

Structural parameters of the computed equilibrium geometries of  $\text{TcX}_4$  [ $X = \text{F}, \text{Cl}, \text{Br}, \text{I}$ ] compounds are given in

**Table 1.** Structural Parameters of  $\text{TcX}_4$  [ $X = \text{F}, \text{Cl}, \text{Br}, \text{I}$ ]

	$\text{TcF}_4$		$\text{TcCl}_4$		$\text{TcBr}_4$		$\text{TcI}_4$
	DFT <sup>a</sup>	DFT <sup>a</sup>	Exp. <sup>b</sup>	DFT <sup>a</sup>	Exp. <sup>c</sup>	DFT <sup>a</sup>	DFT <sup>a</sup>
space group	<i>Pbca</i>	<i>Pbca</i>	<i>Pbca</i>	<i>Pbca</i>	<i>Pbca</i>	<i>Pbca</i>	$P2_1/c$
Lattice							
$a$ (Å)	10.01	12.15	11.65(1)	12.82	12.1777(9)	13.18	
$b$ (Å)	11.92	14.68	14.06(1)	15.25	14.7397(11)	16.21	
$c$ (Å)	5.60	6.29	6.03(1)	6.53	6.3237(5)	6.93	
$b/a$	1.19	1.21	1.21	1.19	1.21	1.23	
$c/a$	0.56	0.52	0.52	0.51	0.52	0.53	
Distance <sup>d</sup> (Å)							
Tc(1)–X(1)	1.87	2.26	2.24	2.41	2.40	2.62	
Tc(1)–X(2)	1.87	2.26	2.25	2.41	2.40	2.63	
Tc(1)–X(3)	2.02	2.38	2.38	2.52	2.53	2.71	
Tc(1)–X(4)	2.05	2.45	2.49	2.61	2.62	2.79	
Tc(1)–X(5)	2.05	2.45	2.49	2.61	2.63	2.80	
Tc(1)–X(6)	2.02	2.38	2.39	2.52	2.53	2.70	
Tc(1)–Tc(2)	3.32	3.77	3.62	3.94	3.79	3.88	
Angle <sup>d</sup> (deg)							
X(1)–Tc(1)–X(2)	98.1	94.3	94.1	94.5	94.3	93.4	
X(1)–Tc(1)–X(3)	98.9	91.8	89.9	91.5	91.5	89.8	
X(1)–Tc(1)–X(4)	167.7	168.5		170.2	175.0	169.5	
X(1)–Tc(1)–X(5)	88.9	90.7	89.7	90.5	89.7	91.0	
X(1)–Tc(1)–X(6)	92.1	98.0	94.0	97.6	94.0	99.6	
X(5)–Tc(1)–X(6)	70.6	77.3	84.3	79.4	85.1	80.4	
X(5)–Tc(2)–X(6)	70.6	77.3		79.5	85.2	89.6	
Tc(1)–Cl(5)–Tc(2)	109.4	102.7	95.6	100.4	94.7	96.6	
Tc(1)–Cl(6)–Tc(2)	109.4	102.7	95.9	100.6	94.9	93.1	

<sup>a</sup>This work. <sup>b</sup>Crystallographic data from Elder and Penfold (1966). Standard errors in bond lengths and angles are 0.006–0.007 Å and 0.3°. <sup>c</sup>Crystallographic data from Poineau et al. (2009). Standard errors in bond lengths and angles are 0.00004 Å and 0.00011–0.00013°. <sup>d</sup>Labeling of the atoms according to the layout in Figure 1c.

Table 1, along with XRD data for  $\text{TcCl}_4$ <sup>6</sup> and  $\text{TcBr}_4$ .<sup>13</sup> Calculations show that  $\text{TcF}_4$  is isomorphous with  $\text{TcCl}_4$  and  $\text{TcBr}_4$  crystals, that is, orthorhombic with the centrosymmetric space group  $Pbc_a$ , while  $\text{TcI}_4$  crystallizes in the monoclinic space group  $P2_1/c$ . The calculated unit cell dimensions  $a$  ( $X$  axis),  $b$  ( $Y$  axis), and  $c$  ( $Z$  axis) are 10.01,

(17) Delley, B. *J. Chem. Phys.* **2000**, *113*, 7756.

(18) Wang, Y.; Perdew, J. P. *Phys. Rev. B* **1992**, *45*, 13244.

(19) Hehre, W. J.; Radom, L.; Schleyer, P. R.; Pople, J. A. *Ab Initio Molecular Orbital Theory*; Wiley: New York, 1986.

(20) Monkhorst, H. J.; Pack, J. D. *Phys. Rev. B* **1976**, *13*, 5188.

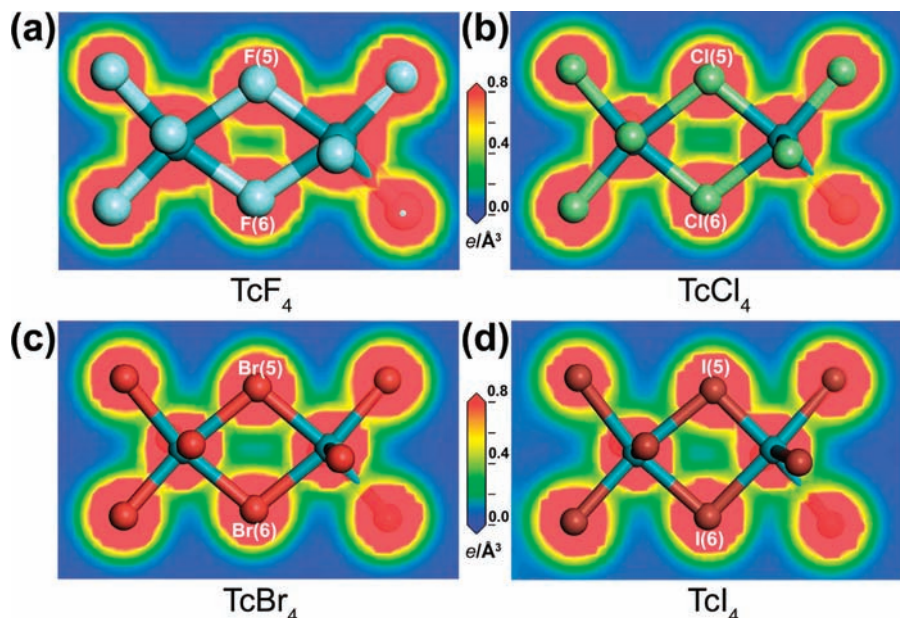


**Figure 2.** Electronic charge densities of (a)  $\text{TcF}_4$ , (b)  $\text{TcCl}_4$ , (c)  $\text{TcBr}_4$ , and (d)  $\text{TcI}_4$  chains projected onto the plane containing the  $\text{Tc-X-Tc}$  double bridge. Charge densities are plotted in  $e/\text{\AA}^3$  units.

11.92, 5.60  $\text{\AA}$  for  $\text{TcF}_4$ , 12.15, 14.68, 6.29  $\text{\AA}$  for  $\text{TcCl}_4$ , 12.82, 15.25, 6.53  $\text{\AA}$  for  $\text{TcBr}_4$ , and 13.18, 16.21, 6.93  $\text{\AA}$  for  $\text{TcI}_4$ , respectively. Relaxed unit cells for  $\text{TcCl}_4$  and  $\text{TcBr}_4$  crystals are systematically larger than experimental lattice constants, although the calculated  $b/a$  and  $c/a$  ratios are in excellent agreement with experimental values. No significant variation of these ratios is observed along the Tc tetrahalide series, with values in the vicinity of  $b/a \sim 1.20$  and  $c/a \sim 0.52$ . The calculated unit cell parameter  $c$ , varying along the chain direction, increases linearly with the effective ionic radius of the halogen ion with formal charge  $-1$ , that is,  $r_{\text{F}} = 1.33 \text{ \AA}$ ,  $r_{\text{Cl}} = 1.81 \text{ \AA}$ ,  $r_{\text{Br}} = 1.96 \text{ \AA}$ , and  $r_{\text{I}} = 2.20 \text{ \AA}$ .<sup>21</sup>

The computed interchain contact distances are in the ranges 3.10–3.48  $\text{\AA}$  for  $\text{F}\cdots\text{F}$ , 3.67–4.14  $\text{\AA}$  for  $\text{Cl}\cdots\text{Cl}$ , 3.54–4.23  $\text{\AA}$  for  $\text{Br}\cdots\text{Br}$ , and 3.36–4.34  $\text{\AA}$  for  $\text{I}\cdots\text{I}$ , in fair agreement with the sum of recommended crystallographic van der Waals radii<sup>22</sup> of F, Cl, Br, and I, that is, 3.0, 3.6, 3.8, and 4.2  $\text{\AA}$ , respectively. The absence of explicit van der Waals interaction terms in our calculations limits the interchain  $\text{X}\cdots\text{X}$  attraction forces, resulting in a systematic antagonistic increase and decrease of the  $\text{Tc-X-Tc}$  and  $\text{X-Tc-X}$  angles, respectively, in the bridge rhomboids compared to experiment. These angular deformations translate into a 4% elongation of the  $\text{Tc-Tc}$  distances in  $\text{TcCl}_4$  (3.77  $\text{\AA}$ ) and  $\text{TcBr}_4$  (3.94  $\text{\AA}$ ) relative to XRD data. The  $\text{Tc-Tc}$  distances in  $\text{TcF}_4$  and  $\text{TcI}_4$  chains are 3.32  $\text{\AA}$  and 3.88  $\text{\AA}$ , respectively.

Three pairs of chemically distinct  $\text{Tc-X}$  bonds are found in all four compounds, with mean bond lengths of 1.87, 2.02, 2.05  $\text{\AA}$  in  $\text{TcF}_4$ , 2.26, 2.38, 2.45  $\text{\AA}$  in  $\text{TcCl}_4$ , 2.41, 2.52, 2.61  $\text{\AA}$  in  $\text{TcBr}_4$ , and 2.62, 2.70, 2.79  $\text{\AA}$  in  $\text{TcI}_4$ . The shortest length corresponds to the bonds between Tc and the non-bridging X atoms; the two largest bond lengths are found in the bridge rhomboids and are close to the sum of the effective ionic radii<sup>21</sup> of Tc and X with formal charges  $+4$  and  $-1$ , respectively:  $r_{\text{Tc}} + r_{\text{F}} = 1.98 \text{ \AA}$ ,  $r_{\text{Tc}} + r_{\text{Cl}} = 2.45 \text{ \AA}$ ,  $r_{\text{Tc}} + r_{\text{Br}} = 2.61 \text{ \AA}$ , and  $r_{\text{Tc}} + r_{\text{I}} = 2.85 \text{ \AA}$ . Computed  $\text{Tc-Br}$  bond lengths

**Table 2.** Calculated Hirshfeld atomic charges (in  $e$ ) in  $\text{TcX}_4$  [ $X = \text{F, Cl, Br, I}$ ]

	$\text{TcF}_4$	$\text{TcCl}_4$	$\text{TcBr}_4$	$\text{TcI}_4$
Tc	+0.51	+0.07	-0.05	-0.19, -0.22
X(bridge)	-0.12	+0.01	+0.04	+0.07, +0.09
X(terminal)	-0.13	-0.04	-0.02	+0.01, +0.03

reproduce recent XRD data<sup>13</sup> with an accuracy better than 0.5%, while calculated  $\text{Tc-Cl}$  bond lengths agree with experimental values<sup>6</sup> within  $\sim 1\%$ .

Partial charges calculated using the Hirshfeld partitioning of the electron density are reported for Tc tetrahalide compounds in Table 2. The charge carried by Tc atoms varies gradually from  $+0.51 e$  for  $\text{TcF}_4$  to  $-0.22 e$  for  $\text{TcI}_4$ , as the electronegativity of the surrounding halogen atoms decreases and the atomic radius increases down the halogen series. In the  $\text{TcF}_4$  and  $\text{TcCl}_4$  chains, the Tc atoms donate electronic charge to halogens, while charge is transferred to Tc atoms in  $\text{TcBr}_4$  and  $\text{TcI}_4$ . Charge transfer between Tc and halogen atoms is relatively modest for  $\text{TcCl}_4$  and  $\text{TcBr}_4$  compared to  $\text{TcF}_4$  and  $\text{TcI}_4$ . Terminal halogen atoms show a tendency to be slightly more electron-withdrawing than halogen atoms bridging Tc atoms. These findings are further confirmed in Figure 2 depicting the projected electronic charge densities of  $\text{TcX}_4$  chains projected onto the plane containing the  $\text{Tc-X-Tc}$  double bridge. Except for  $\text{TcI}_4$ , the calculated charge densities appear continuous along terminal halogens and Tc atoms, explaining the shorter bond lengths of  $\text{Tc}(1)-\text{X}(1)$  and  $\text{Tc}(1)-\text{X}(2)$  relative to bridge  $\text{Tc-X}$  bonds. The charge density distribution in  $\text{TcF}_4$  chains is also uninterrupted along the shortest pair of bonds in the bridge rhomboid, that is,  $\text{Tc}(1)-\text{F}(6)$  and  $\text{Tc}(1)-\text{F}(3)$ . Asymmetry is observed in the charge density of  $\text{TcI}_4$ , accounting for some of the structural distortion in this compound with  $P2_1/c$  symmetry.

Figure 3 displays the computed total and orbital-projected densities of states (DOS) of the  $\text{TcX}_4$  [ $X = \text{F, Cl, Br, I}$ ] compounds. DOS calculations show metallic characteristics for all four Tc tetrahalides. Valence and conduction peaks near

(21) Shannon, R. D. *Acta Crystallogr.* **1976**, *A32*, 751.

(22) Batsanov, S. S. *Inorg. Mater.* **2001**, *37*, 871.

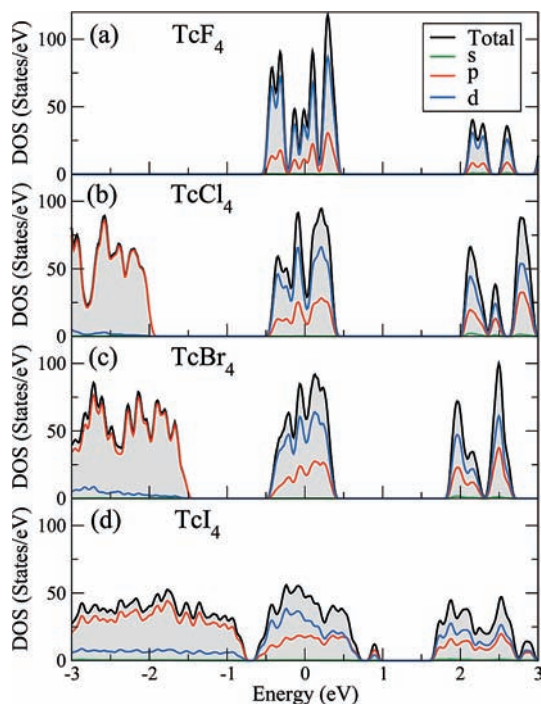


**Figure 3.** Total and orbital-projected densities of states of technetium (IV) halide crystals: (a)  $\text{TcF}_4$ ; (b)  $\text{TcCl}_4$ ; (c)  $\text{TcBr}_4$ ; (d)  $\text{TcI}_4$ . The Fermi energy is set to zero.

the Fermi level ( $E_F$ ) are dominated by Tc 4d orbitals, strongly hybridized with p orbitals from halogens to form  $\sigma$  bonds. Only a small contribution from s orbitals appears in the DOS near  $E_F$  for these chains made of octahedral units with  $d^2sp^3$  hybridization. The calculated total electron densities of states at the Fermi surface are 46.4, 37.3, 61.8, and 47.1 states/eV for  $\text{TcF}_4$ ,  $\text{TcCl}_4$ ,  $\text{TcBr}_4$ , and  $\text{TcI}_4$ , respectively. Peaks at the bottom of the valence band are dominated by p-orbital contributions from halogens, while d-orbital character plays only a minor role. As the number of molecular states increases

from  $\text{TcF}_4$  to  $\text{TcI}_4$ , energy gaps between peaks in the vicinity of the Fermi level and other peaks in the conduction and valence bands get narrower, and molecular features tend to fade out because of the more efficient orbital overlap.

### Conclusion

Using all-electron spin-polarized DFT, we have predicted the existence of  $\text{TcF}_4$  and  $\text{TcI}_4$  compounds and studied the crystal and electronic structures of  $\text{TcX}_4$  [ $X = \text{F}, \text{Cl}, \text{Br}, \text{I}$ ] compounds. Isomorphous with  $\text{TcCl}_4$  and  $\text{TcBr}_4$  crystals,  $\text{TcF}_4$  is orthorhombic with the centro-symmetric space group  $Pbca$ , while  $\text{TcI}_4$  crystallizes in the monoclinic space group  $P2_1/c$ . These Tc tetrahalides consist of distorted *cis* edge-sharing bioctahedra linked into endless chains,  $[\text{TcX}_2(\mu\text{-X})_4]_{\infty}$ . Calculated structural data for the chains are in close agreement with available XRD data for  $\text{TcCl}_4$  and  $\text{TcBr}_4$ . Population analysis shows that the charge carried by Tc atoms varies gradually from  $+0.51 e$  for  $\text{TcF}_4$  to  $-0.22 e$  for  $\text{TcI}_4$ , as the electronegativity of the surrounding halogen atoms decreases and the atomic radius increases down the halogen series. Density-of-states (DOS) calculations show metallic characteristics for all four Tc tetrahalides, with valence and conduction peaks near the Fermi level dominated by Tc 4d orbitals, strongly hybridized with p orbitals from halogens to form  $\sigma$  bonds. Furthermore, molecular features in the DOS gradually fade out as the number of molecular states increases from  $\text{TcF}_4$  to  $\text{TcI}_4$ .

Experimental efforts to synthesize and characterize the two remaining Tc(IV) halides are underway.

**Acknowledgment.** Funding for this research was provided by the U.S. Department of Energy, agreement no. DE-FG52-06NA26399.

**Supporting Information Available:** Structural data in CIF format for  $\text{TcX}_4$  [ $X = \text{F}, \text{Cl}, \text{Br}, \text{I}$ ] crystals, basis sets used in the calculations, and structural optimization details. This material is available free of charge via the Internet at <http://pubs.acs.org>.